A continuous wave transmission method for the ultrasonic spectrometry of liquids

1998 Meas. Sci. Technol. 9 1266

(http://iopscience.iop.org/0957-0233/9/8/020)

Meas. Sci. Technol. **9** (1998) 1266–1276. Printed in the UK PII: S0957-0233(98)88746-8

A continuous wave transmission method for the ultrasonic spectrometry of liquids

J Schultz and U Kaatze

Drittes Physikalisches Institut, Georg-August-Universität, Bürgerstraße 42–44, D-37073 Göttingen, Germany

Received 27 October 1997, in final form 18 February 1998, accepted for publication 22 April 1998

Abstract. A new variable-pathlength method that allows the ultrasonic attenuation coefficient of liquids to be precisely measured as a function of frequency is presented. Focusing on the effect of the sample liquid on the transfer function for continuous acoustical waves, this automated method is particularly useful because of its simple and easy-to-handle electronic set-up, essentially consisting of a computer-controlled network analyser only. The measuring procedure is described and constructional details of the specimen cell are shown. Possible sources of systematic errors are discussed together with depiction of some representative results. It is also explained how the usable frequency range of measurements can be extended towards lower frequencies by operating the apparatus at a fixed pathlength in the resonator mode.

Keywords: acoustical spectroscopy, ultrasonic attenuation, chemical kinetics, molecular dynamics, liquid properties

1. Introduction

Ultrasonic spectrometry has proven a powerful technique for studying elementary chemical and physical processes in liquids. Among the mechanisms that are successfully investigated with this method are various types of reactions, such as dimerization and higher-order association, hydrolysis and protolysis, conformational changes and complex formation and aggregation (Tamm 1961, Eigen and De Maeyer 1963, Slutsky 1981, Stuehr 1986, Strehlow 1992). Additionally examined are density fluctuations (Herzfeld and Litovitz 1959, Litovitz and Davis 1965), fluctuations in the concentration, including critical systems (Dunker *et al* 1983, Fast and Yun 1988, Davidovich *et al* 1990, Brai and Kaatze 1992, Bittmann *et al* 1994, Menzel *et al* 1997) and also thermal, viscous and higher-order boundary effects in micro-heterogeneous liquids, particularly in suspensions and emulsions (Javanaud *et al* 1986, McClements 1992, Schröder and Raphael 1992, Farrow *et al* 1995, Kaatze *et al* 1996). Owing to the versatility of the method, the interest in ultrasonic spectrometry springs not just from fundamental studies in chemistry and condensed matter physics but also from a multitude of applications, especially in chemical engineering and automated process control.

Acoustical methods in use to measure the sonic attenuation coefficient α of liquids as a function of the frequency ν cover roughly the range 10^5–10^{10} Hz (Eggers and Kaatze 1996). These methods are subdivided into two groups, resonator techniques and pulse-modulated propagating wave transmission techniques. The former method is matched to the lower part of the aforementioned frequency range, for which the sonic attenuation coefficient of liquids is normally small (figure 1). In resonator cells the effective path of interaction of the sonic wave with the sample liquid is substantially lengthened by multiple reflections. At higher frequencies, for which $\alpha x_s > 1$ (x_s is the sample thickness), a propagating wave method is appropriate insofar as the amplitude of the acoustic signal is noticeably reduced on the signal's passing just once the liquid column of reasonable length x_s. In order to simplify the evaluation procedure, pulsed modes of operation are used throughout so that the somewhat misleading term 'pulse method' has become widely established. Owing to the large difference between the propagation velocities of acoustic and electromagnetic waves, the discrimination of the sonic signals from the omnipresent undesired electrical cross talk is made possible by the use of pulse-modulated waves and it is also possible to separate the direct acoustic signal from reflected waveforms that, in some cases, might be also present.

These well-tried methods have been applied widely with much success in the past and are still generally accepted today. Nevertheless, both methods are subject to some drawbacks. Since a calibration procedure to determine the inherent instrumental loss is necessary, resonator techniques allow for the measurement of α

0957-0233/98/081266+11$19.50

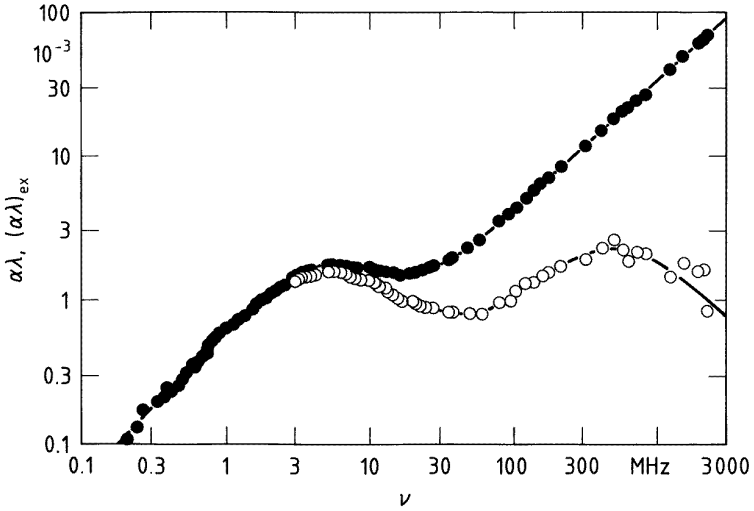

Figure 1. The ultrasonic attenuation per wavelength, $\alpha\lambda$, displayed as a function of the frequency ν for a 0.1 molar aqueous solution of $MnSO_4$ at 25 °C (•), (Eggers and Funck 1973, Kaatze *et al* 1987, Behrends *et al* 1996). Here λ is the sonic wavelength within the liquid. The circles indicate the excess absorption $(\alpha\lambda)_{ex}$. The excess absorption spectrum, obtained from the total attenuation spectrum by subtraction of a background part proportional to ν, is due to the incomplete dissociation of manganese sulphate in water (Tamm 1961). Data are from resonator measurements (0.1–10 MHz), from measurements using pulse-modulated propagating wave transmission techniques (10–3000 MHz), and from ones utilizing pulse-modulated waves in combination with fixed-path cells (5–50 MHz).

relative to the attenuation coefficient of a reference liquid only. The need for a calibration is a severe disadvantage in broad-band spectrometry. It is not just the attenuation coefficient of the reference that has to be precisely known. In addition, the velocity of sound and density of the reference liquid should also as closely as possible agree with the corresponding sample data (Eggers and Kaatze 1996, Eggers 1997). Besides such strict demands for a careful choice of the reference liquid there are also rigorous requirements on the mechanical stability of the resonator cell, which should maintain its delicate adjustment during the emptying, cleaning and refilling procedure when the sample is exchanged for the reference. This is true even though somewhat less stability is required if the focusing action of convexo-concave lenses (Kononenko 1987) or of concave reflectors (Behrends *et al* 1996) is utilized.

The pulse-modulated propagating wave techniques normally involve variable-pathlength cells and thus allow for an absolute determination of the attenuation coefficient α. However, the pulsed mode of operation requires a rather complicated electronic set-up. A particular disadvantage is the need for a receiver with a sufficiently broad detection bandwidth to allow the signals to pass without too unfavourable a distortion of the pulse shape. The sensitivity of the receiving unit is limited thereby so that, under normal conditions, a broad-band RF power amplifier is needed in order to enhance the amplitude of the signal exciting the liquid.

So far we have considered the most commonly applied methods of ultrasonic attenuation coefficient measurements. In these methods either the use of CW signals is combined with fixed-path (resonator) techniques or pulse-modulated signals are applied to operate variable-pathlength cells. Another alternative is the combination of pulse-modulated waves with fixed-path cells, which has been used in the frequency range about 1–150 MHz (Eggers and Funck 1973, Kaatze *et al* 1988). However, the fixed-pathlength pulse-modulated propagating wave method combines the unfavourable characteristics of both of the aforementioned methods, namely the need for reference measurements for determination of the cell's length and the necessity of a sophisticated electronic set-up for the proper processing of the pulsed signal (Eggers and Kaatze 1996). Here we aim to develop a measuring method which is based on the remaining fourth signal–cell-type combination that has not been used so far.

Especially for liquids near a critical point, propagating wave measurements at low input power level appear to be most desirable. Such methods should utilize highly sensitive receiver systems of small intermediate-frequency (IF) bandwidth. Hence the methods should be based on continuous wave (CW) signals. If this idea is accepted then the more complicated transfer function of the cell, potentially containing contributions from multiple reflections and also from electrical cross talk, has to be analysed. Since nowadays computing facilities promise such analysis with sufficient accuracy we decided to develop a CW method that uses a variable-pathlength cell. In order to allow the data recording and evaluation procedures to be made as simple as possible, suitable also for industrial test and control routines, we restricted the electronic set-up to a commercial network analyser combined with a laboratory computer.

In practice it is often found that measurements in the frequency range roughly 1–50 MHz, for which in principle both resonator and pulse-modulated propagating wave methods are appropriate, are difficult to perform with the desired precision. This is particularly true for many interesting aqueous systems, due to the unfavourable α values in that frequency range. On the one hand, α values

may be so high that the resonance curves of resonator cells become too broad to be unambiguously separable from spurious higher-order satellite peaks or even from neighbouring resonance curves. On the other hand, the attenuation coefficient may nevertheless be too small to result in an amplitude variation of the signal passing the liquid column that is sufficiently strong to allow accurate 'pulse' measurements. We thus focused especially on methods of measuring the attenuation coefficient in this intermediate-frequency range. Our procedure differs from that recently proposed by Eggers and Richmann (1993), who developed another method of analytical elimination of cross talk but concentrated on higher frequencies, for which the attenuation coefficient is normally so high that multiple reflections of the acoustic signal can be neglected.

2. Principles of the method

Consider a liquid column of variable length x_s, placed between two disc-shaped piezoelectric transducers, one located at $x = 0$, to be operated as a transmitter, and the other one at $x = x_s$, to be used as a receiver (figure 2). For reasons of simplicity let us first assume infinite lateral dimensions of the transducers and of the sample column as well. The acoustic reflection coefficients at the transmitter/liquid and liquid/receiver interfaces may be denoted by r_t and r_r, respectively. Both transducers are assumed to be backed by air. Hence, due to the finite thickness of the transducers, the reflection coefficients r_t and r_r depend on the frequency ν of the sonic signal. The acoustic transfer function T_{ac} of the specimen cell is then given by the relation

$$T_{ac}(\nu, \alpha, c_s, x_s) = \hat{T}_{ac}\frac{(1 + r_r(\nu))\exp(-\gamma x_s)}{1 - r_t(\nu)r_r(\nu)\exp(-2\gamma x_s)} \qquad (1)$$

where c_s denotes the velocity of sound in the sample liquid and

$$\gamma = \alpha + \mathrm{i}2\pi\nu/c_s \qquad (2)$$

is the propagation constant of the sonic wave ($\mathrm{i}^2 = -1$). In equation (1) $\hat{T}_{ac}$ is an amplitude.

In the pulse-modulated mode of measurements the sample cells are often operated under conditions that allow equation (1) to be approximated by the simple relation

$$T_{ac}(\nu, \alpha, c_s, x_s) = \hat{T}_{ac}(1 + r_r)\exp(-\alpha x_s) = \tilde{T}_{ac}\exp(-\alpha x_s) \qquad (3)$$

where $\tilde{T}_{ac} = \hat{T}_{ac}(1 + r_r)$.

Equation (3) can be used either at high sample loss ($\alpha x_s > 3$) or with a pulse duration τ_p that is sufficiently small to prevent reflected waveforms from undergoing superposition with the direct signal ($\tau_p < 2x_s/c_s$). If, as another extreme, the attenuation coefficient of the sample is small ($\alpha x_s < 0.1$), standing wave contributions dominate the acoustic field properties. Fixed-path cells are used in such conditions and operated as resonator interferometers (Eggers and Kaatze 1996). The transfer function (equation (1)) is then developed in terms of the variation in frequency around the frequencies of cell resonances, as will be discussed below (section 6).

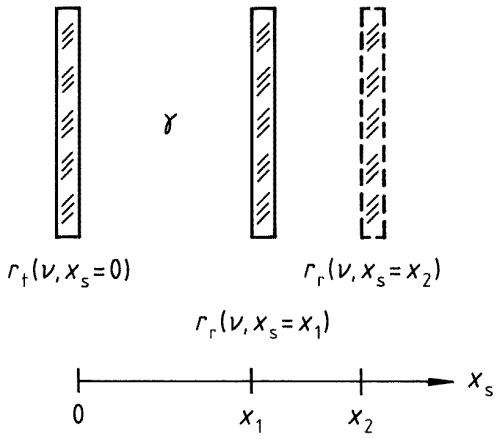

Figure 2. A sketch of the variable-sample-length cell.

In the continuous wave transmission method described in this paper the total transmission function $T_{tot} = U_r/U_t$ of the apparatus (U_r and U_t are the receiver and transmitter voltages, respectively) will typically also contain contributions from electrical cross talk, $\hat{C}\exp(\mathrm{i}\phi_c)$. On the other hand, identical piezoelectric transmitter and receiver crystals are normally used so that $r_t = r_r := r(= \hat{r}\exp(\mathrm{i}\phi_r))$ is a realistic assumption. Hence

$$|T_{tot}| = \left|\hat{T}_{ac}\frac{(1 + r(\nu))\exp(-\gamma x_s)}{1 - r^2(\nu)\exp(-2\gamma x_s)} + \hat{C}\exp(\mathrm{i}\phi_c)\right|. \qquad (4)$$

This relation corresponds to the transfer function of microwave interferometers designed to measure the dielectric spectrum of liquids (Kaatze *et al* 1995). From a physical point of view, however, there is an important difference between the transfer functions of the two spectroscopic methods. In the microwave (double-beam) interferometry the second term on the right-hand side of equation (4) represents a reference signal that can be precisely adjusted to yield maximum sensitivity in the measurements. In acoustic spectrometry this term describes an undesired disturbing signal. In order that it does not affect ultrasonic measurements too adversely, it has to be sufficiently suppressed by suitable provisions such as electrical shielding. If, however, the amplitude ratio $\hat{C}/\hat{T}_{ac}$ does not adopt values that are too unfavourable, separation of the electrical cross talk from the desired cell signal is possible due to the independence of the phase ϕ_c from x_s which results from the large difference in the propagation velocities (and thus wavelengths) for electromagnetic and sonic waves (see below for the possible dependence of $\hat{C}$ upon x_s). An example of a measured total transfer function is shown in figure 3, in which the magnitude $|T_{tot}|$ is displayed versus the cell length x_s. A plot from a hypersonic cell operated at around 4.5 GHz has been chosen here to illustrate the wide applicability of the method. It can also nicely be seen from this plot that, at small x_s, for which multiple reflections within the sample cell contribute to the receiver signal, the $\lambda_s/2$ periodicity following from the acoustic signal term in equation (4) is in fact found in the transfer function whereas at larger x_s the superposition

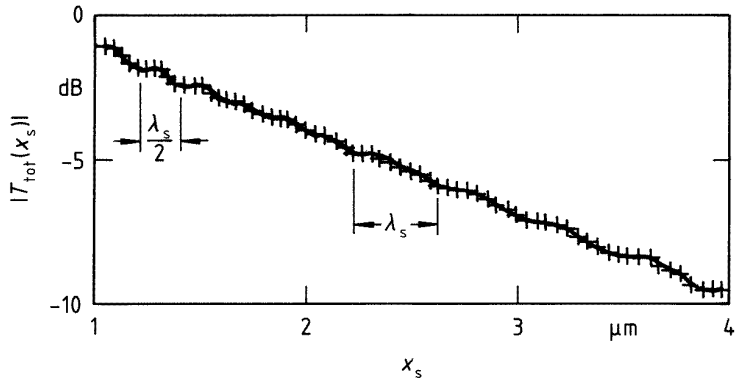

Figure 3. The amplitude of the signal transmitted through a hypersonic cell displayed as a function of the cell's length x_s (+). The full curve is the graph of the amount $|T_{tot}|$ of the transmission function defined by equation (4) with parameter values found in a nonlinear least squares regression analysis. Here ν = 4.553 GHz, c_s = 1853 m s^{-1}, $\alpha = 4.8 \times 10^5$ m^{-1}, r = 0.49 and $\hat{C}/\hat{T}_{ac} = 3.3 \times 10^{-3}$ (Kühnel 1995).

of the reduced acoustic signal with the cross talk leads to a structure with λ_s periodicity. Here $\lambda_s = c_s/\nu$ denotes the sonic wavelength within the sample. Hence the differences in x_s values at which relative maxima or minima in $|T_{tot}|$ exist are closely related to the acoustic wavelength λ_s and, therefore, to the velocity of sound c_s in the sample at the frequency ν so that c_s can be determined from the measurements. The amplitude ratio of successive relative maxima reflects the attenuation coefficient α of the liquid. Additionally unknown (but less interesting) parameters that have to be found by fitting equation (4) to sets of measured transfer function data are the magnitude and phase of the complex reflection coefficient r, the amplitude ratio $\hat{C}/\hat{T}_{ac}$ and the constant phase angle ϕ_c of the cross talk signal.

3. The cell's design and the electronic apparatus

The construction of the cell used in this study resembles that of previously described cells for pulse-modulated measurements at variable sample length (Kaatze *et al* 1988, 1993). A sketch of the cell's design and an equivalent circuit diagram of the electronic apparatus is given in figure 4. The sample (1) rests in a container made of glass or plexiglass (2) that is surrounded by a jacket for circulating thermostat fluid (3). Two piezoelectric transducers (4a and b) are immersed in the sample liquid; one is operated as transmitter (4a) and the other one as a receiver (4b). We used circular cylindrical quartz discs, 60 mm in diameter, with a longitudinal fundamental frequency $\nu_T = 0.5$ MHz (transducer thickness 5.7 mm) here. The transducers were stuck into their fixtures (6a and b) with the aid of silicone rubber (5a and b). In order to provide electrical contact of the transducer discs, layers of chrome and gold were evaporated onto their front and rear sides, respectively. Zigzag-shaped copper stripes are embedded in the silicon rubber in order to ground the front side. Contact of the transducer's back side is established via sprung bronze contacts (7a and b). In order to guarantee strict parallelism of the transducer's front sides to one another the axis of the sample container, with the aid of three suitable screws (8), can be adjusted with respect to the axis of the receiver transducer (4b). The fixture of that transducer is mounted on a sliding carriage (9). Smooth and backlash-free shifting of this movable plate (9) and thus of the receiver transducer (4b) is allowed by high-precision ball–bush guides (10). The position of the sliding carriage, driven by a stepping motor (11), is measured by an optical distance meter (12, Heidenhain, Traunreut, Germany) with a resolution of 0.1 μm. The absolute accuracy of the instrument is 1 μm. The smallest step in the adjustment of the transducer spacing is 0.1 μm here. The reproducibility in the positioning of the shiftable transducer is also 0.1 μm. At the highest frequency under consideration (50 MHz), assuming that $c_s = 1500$ m s^{-1} is the velocity of sound in a typical sample liquid, this corresponds to an accuracy of better than to within $3 \times 10^{-3}\lambda_s$ in the sample length x_s.

The transmitter quartz disc is driven at ν_T and the odd overtones $(2n + 1)\nu_T$ of its fundamental frequency. The CW signal (S) is provided by the synthesized generator of a network analyser (NWA, 13). Part of this signal is fed back to the reference input (R) of the NWA. The transmitter's driving signal may be first amplified by a broadband amplifier (14) in order to enhance the signal-to-noise ratio in the measurements. When the signal has passed the cell it is received by the measuring input (M) of the NWA and finally stored in a laboratory computer (15) which also receives the signal from the forwards/backwards counter (12a) of the distance meter (12). Additionally, the computer controls the stepping motor drive and control unit (11a) and thus the procedure of measuring the transfer function T_{tot}. Various standard network analysers are suitable for these measurements. We used a Hewlett-Packard 8753A instrument, designed for the frequency range 300 kHz to 3 GHz. It is specified to have a dynamic range of 100 dB. Within the present frequency range of measurement (1–50 MHz) the typical accuracy of amplitude ratio measurements is to within better than 0.1 dB and the typical phase deviation from linearity is smaller than 0.3°.

4. Measuring procedures

In figure 5 the section of the standing wave pattern of the sonic CW field is shown that results if the signal

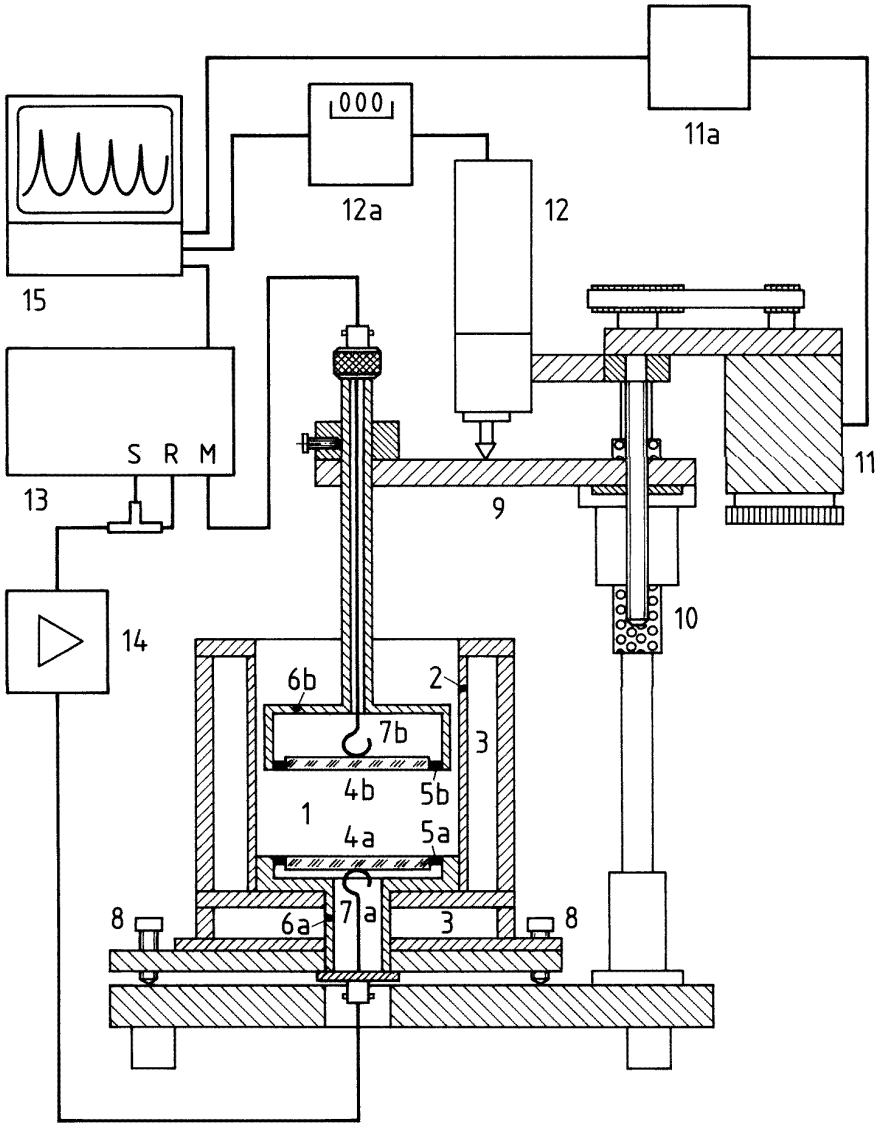

Figure 4. The construction of the specimen cell and the block diagram of the electronic apparatus: 1, sample volume; 2, cell jacket made of glass or plexiglass; 3, channels for circulating thermostat fluid; 4, transmitter (4a) and receiver (4b) piezoelectric transducers; 5a and 5b, sealing layers of silicone rubber with embedded electrical contacts to ground the front side transducer electrodes; 6a and 6b, transducer mounts; 7a and 7b, flexible electrical contact wires connecting the transducer back side electrodes to the electronic circuit; 8, screw for parallel adjustment of the transducer discs; 9, sliding carriage; 10, high-precision ball–bush guide; 11, stepping motor with 11a, control unit; 12, digital distance meter with 12a, forwards/backwards counter; 13, network analyser; 14, broadband amplifier; and 15, laboratory computer.

transmitted through the liquid-filled cell is displayed as a function of the sample length x_s. As indicated by the full curve also given in figure 5 the measured data can be well represented by the $|T_{tot}|$ versus x_s relation defined by equation (4). For the following reasons, it is nevertheless difficult to obtain a precise value of the desired attenuation coefficient α from segments of the transfer function. The attenuation coefficient of the sample liquid is predominantly reflected by the ratio $T_{tot}(x_{s(n+1)})/T_{tot}(x_{sn})$ of successive maximum values of the standing wave pattern (figure 5). On the one hand, a long segment, exhibiting a significant decrease in the maximum values of $|T_{tot}|$, is thus desired in the measurements. On the other hand, it is also necessary to have included in the series of discrete points of measurement some $|T_{tot}|$ data close to the maximum values $|T_{tot}(x_{sn})|$. The latter requirement means that tedious and time-consuming series of data recordings are needed if the x_s values in the measurements are equidistantly distributed over a relevant interval of sample length. This is especially true for liquids with small α. Various strategies to reduce the measuring time significantly have been applied. It was found that a suitable mode of operation consists of performing an initial determination of a short sequence of x_{sn} values at which maximum $|T_{tot}|$ data are found, followed by prediction of further cell lengths $x_{s(n+m)}$ of maximum cell output-to-input signal ratio and by specific measurements at x_s values around those cell lengths. Owing to the electrical cross talk, the x_{sn} values

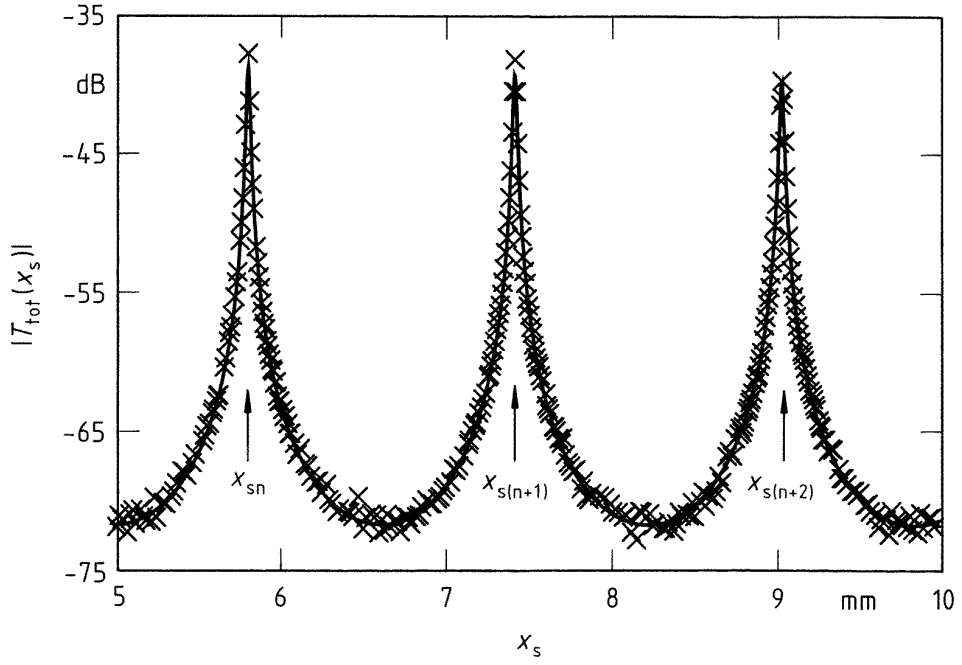

Figure 5. The amplitude of the signal transmitted through the cell as a function of the sample length x_s. The curve is the graph of the $|T_{tot}(x_s|$ function (equation (4)) with parameters found by a fitting procedure. In these measurements the cell was filled with a 0.1 molar aqueous $MnSO_4$ solution at 25 °C (figure 1) and the receiver signal has been probed at equidistant frequency intervals.

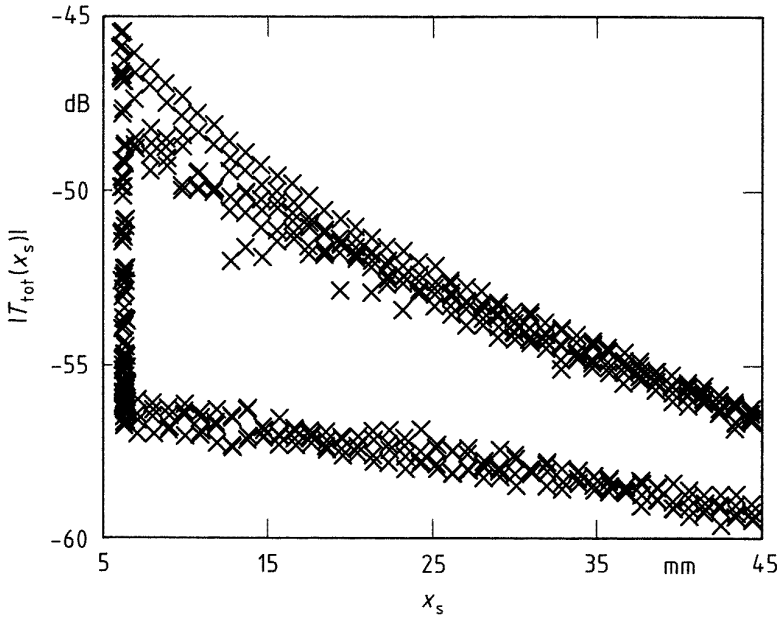

Figure 6. The amplitude of the signal transmitted through the cell displayed as a function of the cell's length x_s. At small cell length ($x_s \approx 6$ mm) some data have been recorded at finely varying x, whereas at larger cell lengths measurements have been performed around predicted x_{sn} values at which T_{tot} adopts relative maxima and also at the x_s values of relative minima in the transmitted signal.

are not strictly equidistantly distributed. Particularly at high frequencies, some corrections in the predicted $x_{s(n+m)}$ data may therefore be necessary. In figure 6, an example for a series of measured $|T_{tot}(x_s)|$ data is displayed to show that the decrease with x_s in the maximum values of the standing wave pattern is adequately considered by this mode of measurements.

It is only briefly mentioned here that the analytical description of the measured transfer function by equation (4) can be improved if the x_s dependence of the amplitude $\hat{C}$

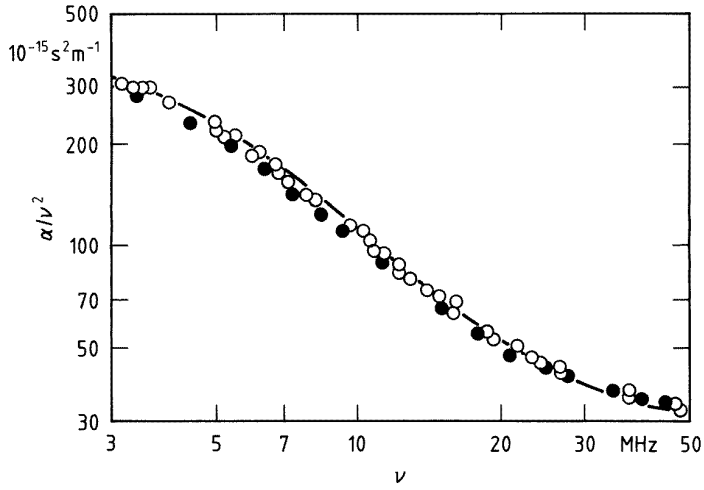

Figure 7. A section of the sonic absorption spectrum of the 0.1 molar aqueous $MnSO_4$ solution (figure 1) in the format α/ν^2 versus ν. Full points refer to measurements with the CW transmission method, circles to reference measurements (figure 1).

of the cross talk is taken into account. This amplitude depends on details of the construction of the feeding lines and sprung contacts to the transducer discs acting more or less as capacitive or inductive electromagnetic antenna. For our cell design the cross talk signal, at relevant cell lengths, decreases as $x_s^{-0.6}$ when the transducer spacing of the empty cell is increased.

5. Representative results and experimental errors

In figure 7 part of the sonic absorption spectrum of 0.1 mol/l $MnSO_4$ in water at 25 °C (figure 1) is displayed in the format α/ν^2 as a function of ν. In the relevant frequency range 3–50 MHz the α values of this $MnSO_4$ solution are rather small. Nevertheless, the α/ν^2 data measured according to the continuous wave transmission method fit fairly well the previous data, obtained from measurements with a variety of resonator cells and with cells for pulse-modulated transmission methods as well. It is also realized that the CW data at $\nu < 25$ MHz are systematically smaller (by about 7%) than the α/ν^2 values measured with the well-tried conventional methods.

Another example is presented in figure 8 in which, at frequencies in the range 2–30 MHz, a section of the ultrasonic absorption spectrum of a butoxyethanol–water mixture is shown in the format $(\alpha\lambda_s)_{ex}$ versus ν. Within the frequency range under consideration the α values of this liquid mixture are substantially higher than those of the aqueous $MnSO_4$ solution considered before. Again the data from the present CW measurements fit nicely to those measured with other methods, including resonator techniques as well as variable-pathlength and fixed-path pulse-modulated wave transmission methods. Here systematic deviations of the present CW data from the previously measured α values emerge at frequencies below 5 MHz.

The conclusions from our measurements on liquids of well-known ultrasonic spectra are the following. (i) The scatter in the data from the new CW method is of the same order as the scatter in the pulse-modulated wave transmission data obtained at variable sample thickness ($\pm 1\%$). (ii) It is somewhat smaller than the scatter in the data obtained from resonator measurements in the same frequency range. There are, however, systematic deviations which seem to affect particularly the CW measurements in the lower part of the available frequency range. We therefore focus our interest on these systematic errors in what follows.

Owing to the finite size of the transducer discs, diffraction phenomena become increasingly important in the transmission of sound waves as the wavelength-to-disc surface area ratio increases (Fay 1976/77, Khimunin and Lvova 1983). In the pulse-modulated wave transmission method in which wave segments are considered that passed the sample of length x_s, once only the amplitude of the transmitted signal has been corrected for diffraction using the factor (Kaatze *et al* 1993)

$$f_{diff}(x_s) = \exp\{-[\lambda_s x_s/(2\pi A)]^{1/2}\}^{g(x_s)} \qquad (5)$$

where $\lambda_s = c_s/\nu$ is the wavelength within the liquid and A denotes the effective transducer surface area, which is assumed to be the same for the transmitter and the receiver transducer. For equally sized and carefully adjusted transmitter and receiver transducer discs with coinciding axes, relation (5) with $g(x) \equiv 1$ results from the numerical evaluation of a theoretical treatment of the effect of diffraction (Fay 1976/77) if the transducers are assumed to be embedded in a sample of infinite lateral dimensions. We have experimentally confirmed these theoretical predictions using a tank filled with water and supplied with differently sized transducer pairs that have been operated in the pulse-modulated mode. The lateral dimensions of the actual cells are not large compared with the transducer diameter's so that non-axially propagating field components are partly reflected at the cylindrical cell jacket. The effect of diffraction on the signal transmitted through the cell is reduced, as considered by $0 < g(x_s) < 1$ in equation (5).

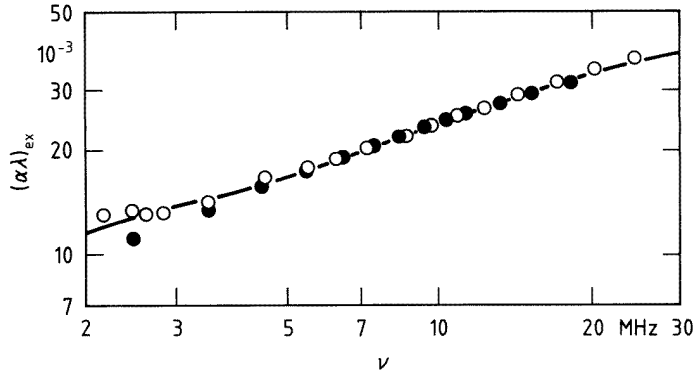

Figure 8. Part of the ultrasonic attenuation spectrum of a butoxyethanol–water mixture (the mole fraction of butoxyethanol is $y = 0.295$) at 25 °C. Full points denote data obtained with this method; circles refer to reference measurements (Menzel *et al* 1997).

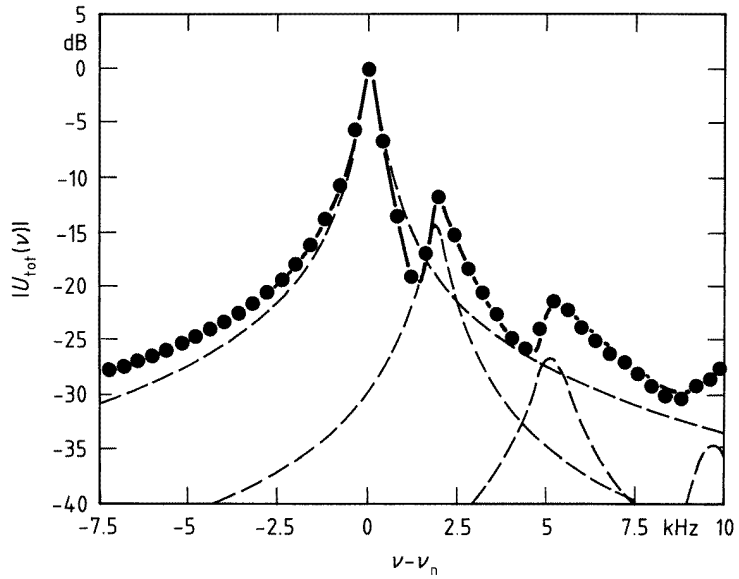

Figure 9. The biplanar (circular cylindrical) resonator's transfer function around the resonance frequency ν_n of a main (longitudinal) resonance (Kühnel 1995). Broken curves are graphs of Lorentz functions; the full curve shows the superposition of these functions; $\nu_n \approx 6$ MHz.

Consideration, of the effect of diffraction according to equation (5) on the transmission function T_{tot} (equation (4)) however, cannot account for the experimental finding of attenuation coefficients smaller than the reference values (figures 7 and 8). For, compared with ideal plane wave propagation, the diffraction effects represented by equation (5) will lead to greater α values, as expected intuitively but in contradiction to our experimental results. Notice, however, that diffraction reduces the amplitude of the signal whenever the wave is reflected at a liquid/transducer interface. For a small sample length x_s more reflections occur than would occur at large x_s values, until the amplitude of the sound field decreases for the same factor. Hence, at low frequencies, for which diffraction effects have a noticeable influence on the sound field, the amplitude of the transmitted signal decreases less strongly with x_s than it would decrease under plane wave conditions in a cell with infinite lateral dimensions. The measured attenuation coefficient values, therefore, appear to be smaller than expected (figures 7 and 8). It is nevertheless possible to calibrate the cell with proper consideration of these diffraction phenomena and to enlarge the frequency range of measurements towards lower frequencies. Measurements in which the sample is replaced by a reference liquid of well-known attenuation coefficient, preferably with matched sound velocity and density, are appropriate for determining the ratio $\alpha_{true}/\alpha_{meas}$ that may be used to correct the measured data for the (small) effect of diffraction. The need for a suitable reference liquid when measurements are extended towards low frequencies is a drawback, but is common to the alternative methods of measurements as well, including the conventional variable-sample-length techniques that use pulse-modulated waves (Kaatze *et al* 1993). With this CW method a noticeable effect of diffraction results, particularly with sample liquids of small attenuation coefficients (figure 7). Hence, for

aqueous systems, like the 0.1 mol/l $MnSO_4$ solution, water can be used as a reference to find the suitable $\alpha_{true}/\alpha_{meas}$ ratio. In doing so the attenuation data from the present continuous wave transmission method are shifted to agree with the literature data to within their accuracy of measurement ($\pm 4\%$ for $\nu < 10$ MHz and $\pm 2\%$ for $\nu > 10$ MHz; Kaatze *et al* (1988) and Behrends *et al* (1996)).

It is only briefly mentioned here that the significance of the parameters in the transfer function $T_{tot}(x_s)$ of the cell can be substantially increased by utilizing also the phase Φ_T of T_{tot}. This is demonstrated by the data displayed in table 1 in which, as an example, parameter values derived from $|T_{tot}(x_s)|$ are compared with those from evaluation both of the magnitude and of the phase of $T_{tot}(x_s)$. It is interesting to notice that the relative difference between the α values obtained from the two modes of evaluation amounts to about 1%. It can also be seen from table 1 that the velocity of sound c_s in the sample results from the transfer function with the small confidence interval $\Delta c_s/c_s = 2 \times 10^{-5}$, or even better if Φ_T is utilized. However, because the resolution of the distance meter used in the measurements is 0.1 μm only, the relative error in the determination of the wavelength $\lambda_s = c_s/\nu$ within the sample is about 0.1 $\mu m/\lambda_s = 1.6 \times 10^{-4}$ at 2.5 MHz. This is an acceptable accuracy for many applications of interest. Resonator methods that are particularly matched to sound velocity measurements at a fixed frequency or within a small frequency range (Sarvazyan 1982, Buckin 1988) allow still higher accuracy and require a much smaller sample volume (<1 ml only).

6. The resonator mode of operation

It is interesting to attempt alternatively to consider the signal transmitted through the cell (equation 4) as a function of the frequency ν rather than of the sample's length x_s. Hence we also used the apparatus sketched in figure 4 to record at constant x_s the resonance curves $|T_{tot}(\nu)|$ of the liquid-filled cavity cell around its resonance frequencies ν_n ($n = 1, 2, 3, \ldots$) and to determine the attenuation coefficient of the sample from the half-power bandwidth $\Delta\nu_{ntot}$ of the resonance at ν_n (Eggers and Kaatze 1996). Because intrinsic cell losses also contribute to $\Delta\nu_{ntot}$ the cell loss contribution $\Delta\nu_{ncell}$ to the total half-power bandwidth has been determined additionally by calibration measurements using a reference liquid of well-known attenuation coefficient. In order to simulate the sound field of the sample-filled cavity resonator as closely as possible, methanol–water mixtures with their velocity of sound and density matched to those of the liquid being tested have been used in the reference measurements throughout.

At small liquid attenuation and small cell losses the transfer function $T_{tot}(\nu)$ around a resonance frequency ν_n can be developed to yield a Lorentzian line shape. The relation

$$\alpha\lambda_s = \frac{\pi}{\nu_n}(\Delta\nu_{ntot} - \Delta\nu_{ncell}) = \pi(Q_{tot}^{-1}(\nu_n) - Q_{cell}^{-1}(\nu_n)) \quad (6)$$

has thus been used as a good approximation in order to determine the attenuation coefficient α of the sample from the quality factors $Q_{tot}(\nu) = \nu_n/\Delta\nu_{ntot}$ and $Q_{cell} = \nu_n/\Delta\nu_{ncell}$.

Table 1. Sets of parameter values together with the experimental errors resulting from fitting measured transfer function data at 2.49 MHz to the $T_{tot}(x_s)$ function (equation (4)). Here $\hat{r}$ and Φ_r are the magnitude and phase, respectively, of the reflection coefficient at the liquid/transducer interfaces: $r(\nu) = \hat{r}\exp(i\Phi_r)$. The parameter Δx_s denotes a small offset in the zero setting of the digital distance meter (12 and 12a in figure 4). The data refer to the cell filled with that butoxyethanol/water mixture at 25 °C, part of the spectrum of which is displayed in figure 8 (for a mass fraction $y = 0.295$ of butoxyethanol).

Parameter	Amount of $T_{tot}(x_s)$ considered only	Amount and phase of $T_{tot}(x_s)$ taken into account
c_s (ms^{-1})	$1495 \pm 0.002\%$	$1495 \pm 0.000\%$
α (m^{-1})	$18.05 \pm 0.2\%$	$18.26 \pm 0.2\%$
$\hat{r}$	$0.78 \pm 2.2\%$	$0.72 \pm 0.06\%$
Φ_r (rad)	$0.99 \pm 1300\%$	$0.95 \pm 0.003\%$
$\hat{C}$ (μV)	$0.33 \pm 6\%$	$0.34 \pm 3.8\%$
Φ_c (rad)	$0.28 \pm 7.6\%$	$-0.83 \pm 0.04\%$
$\hat{T}_{ab}$ (V)	$0.3 \pm 400\%$	$0.18 \pm 0.24\%$
Δx_s (μm)	$0.2 \pm 670\%$	$0.98 \pm 0.005\%$

Owing to the symmetry of the cell's shape the transfer function $T_{tot}(\nu)$, near each main resonance frequency ν_n, exhibits satellite resonances due to radial modes of the sonic field within the circular cylindrical cavity (Labhardt and Schwarz 1976). An example of a typical behaviour of the transfer function around a main (longitudinal) resonance peak with resonance frequency ν_n is displayed in figure 9. To take into account the effect of satellite peaks in the desired resonance frequency ν_n and half-power bandwidth $\Delta\nu_n$ adequately, we always recorded the complex transfer function of the cell around ν_n continuously and, following Trachimow (1994), fitted the results to the sum of a suitable number of Lorentzians afterwards. Both the magnitude and the phase of $T_{tot}(\nu)$ have been utilized in the decomposition of the transfer function and, in the analytical form used in the regression analysis, allowance has been made for the contribution from cross talk and for the effect of the characteristic transducer function on the transfer function of the cell.

An example of attenuation coefficient data measured in the resonator mode of operation of the present set-up (figure 4) is presented in figure 10. These data for the 0.1 molar solution of $MnSO_4$ in water have been obtained from calibrating the cell using a methanol–water mixture as reference in order to measure $Q_{cell}(\nu_n)$ and using pure water at 25 °C in order to determine x_s. Comparison of our results with data from measurements with two specially designed resonator cells (Kaatze *et al* 1987) reveals that the scatter of the present attenuation coefficients is somewhat higher. Notice, however, that, in contrast to the special resonator cells, this cell is provided with rather simple devices for the parallel adjustment of the transducers only. In addition, due to the required provisions for cell length variations, the mechanical stability of the present cell is somewhat smaller than that of cells that are especially designed for resonator measurements. Owing to the multiple reflections

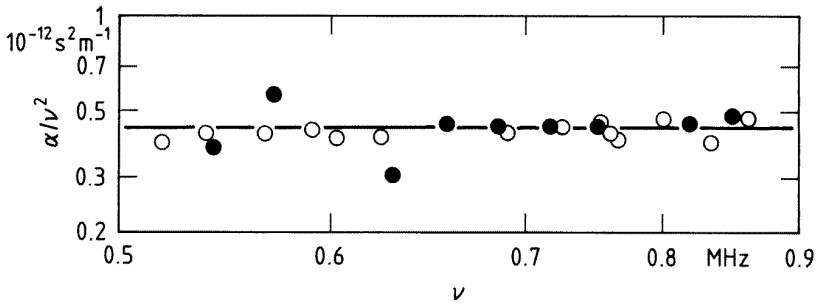

Figure 10. Part of the ultrasonic attenuation spectrum of the 0.1 molar aqueous $MnSO_4$ solution at 25 °C (figure 1). Full points have been measured using the present set-up in the resonator mode of operation; circles indicate reference data (figure 1).

of the waves the resonance curve of a resonator may be affected by extremely small distortions in the cell parameters, such as those resulting, for instance, from structure-borne sound and from spurious displacements of the transducer arrangement when the sample is exchanged for the reference liquid. In a future design of a combined CW transmission/resonator cell these aspects could easily be taken into account.

7. Conclusions

Even though pulse-modulated propagating wave transmission methods allow clear separation of the desired signal from multiply reflected waveforms as well as from the electrical cross talk, thereby allowing precise measurements, the continuous wave transmission method offers a useful alternative. In measurements at frequencies above 1 MHz it allows one to use a much simpler experimental set-up, basically a commercial network analyser, than that of the pulse-modulated propagating wave method. Here we described an apparatus designed for the frequency range 1–50 MHz in which for many systems of interest the attenuation coefficient may be, on the one hand, too large to allow precise resonator measurements but, on the other hand, too small to allow accurate pulse-modulated wave measurements. The continuous wave variable-sample-length method utilizes favourable characteristics of both of the most widely applied conventional methods. Just like in the resonator technique, the effective path of the sonic wave within the sample is noticeably enlarged by multiple reflections. Similarly to the pulse-modulated wave variable-pathlength method, the decrease in the signal's amplitude with increasing sample length is sensitively recorded.

In common with the conventional methods (Behrends *et al* 1996, Kaatze *et al* 1993), diffraction effects may affect the measured data, particularly at low frequencies and at small sample losses. Even under such conditions the method allows one to attain an accuracy of the order of within 1% in the α data if suitable corrections, following from calibration measurements, are applied. Even though, in principle, a reference liquid with its attenuation coefficient, velocity of sound and density matched as closely as possible to those of the properties of the sample should be used, the requirements on the reference are less strong than they are with resonator measurements. Utilizing the same set-up, the usable frequency range of measurement can be additionally enlarged towards lower frequencies merely by switching to a resonator mode of operation. Provisional studies by Kühnel at frequencies in the gigahertz range (figure 3) indicated that CW measurements might be a promising method for use over a very broad frequency range. This prediction, however, has yet to be verified by systematic investigations.

The measurements yield also the velocity of sound c_s in the sample, with its experimental error Δc_s predominantly depending on the accuracy of the distance meter used in the variable-pathlength cell. Here we attained $\Delta c_s/c_s \approx 2 \times 10^{-4}$ at 2.5 MHz using a commercial optical grating distance meter.

Acknowledgments

We thank Drs V Kühnel and T Telgmann for helpful discussions and suggestions and V Kühnel also for making his unpublished results from CW measurements at gigahertz frequencies available to us. Financial support by the Deutsche Forschungsgemeinschaft is gratefully acknowledged.

References

Behrends R, Eggers F, Kaatze U and Telgmann T 1996 Ultrasonic spectrometry of liquids below 1 MHz. Biconcave resonator cell with adjustable radius of curvature *Ultrasonics* **34** 59–67

Bittmann E, Alig I and Woermann D 1994 Ultrasonic absorption of aniline/cyclohexane mixtures of critical and non-critical composition *Ber. Bunsenges. Phys. Chem.* **98** 189–94

Brai M and Kaatze U 1992 Ultrasonic and hypersonic relaxations of monohydric alcohol/water mixtures *J. Phys. Chem.* **96** 8946–55

Buckin V A 1988 Hydration of nucleic bases in dilute aqueous solutions. Apparent molar adiabatic and isothermal compressibilities, apparent molar volumes and their temperature slopes at 25 °C *Biophys. Chem.* **29** 283–92

Davidovich L A, Karabaev M K and Shinder I I 1990 Absorption and velocity of sound near the 'double' critical solution point *Sov. Phys.–Acoust.* **36** 205–6

Dunker H, Woermann D and Bhattacharjee J K 1983 Ultrasonic absorption measurements near the critical point of a reactive binary mixture *Ber. Bunsenges. Phys. Chem.* **87** 591–7

Eggers F 1997 Model calculations for ultrasonic plate–liquid–plate resonators: peak frequency shift by liquid density and velocity variations *Meas. Sci. Technol.* **8** 643–7

Eggers F and Funck Th 1973 Ultrasonic measurements with milliliter liquid samples in the 0.5–100 MHz range *Rev. Sci. Instrum.* **44** 969–77

Eggers F and Kaatze U 1996 Broad-band ultrasonic measurement techniques for liquids *Meas. Sci. Technol.* **7** 1–19

Eggers F and Richmann K H 1993 Ultrasonic absorption measurements in liquids above 100 MHz with continuous waves, employing algebraic crosstalk elimination *Acustica* **78** 27–35

Eigen M and De Maeyer L 1963 Relaxation methods *Technique of Organic Chemistry* vol 8, pt 2, ed A Weissberger (New York: Interscience)

Farrow C A, Anson L W and Chivers R C 1995 Multiple scattering of ultrasound in suspensions *Acustica* **81** 402–11

Fast S J and Yun S S 1988 Critical behaviour of the ultrasonic attenuation for the binary liquid mixture: methanol and cyclohexane *J. Acoust. Soc. Am.* **83** 1384–7

Fay R 1976/77 Numerische Berechnung der Beugungsverluste im Schallfeld von Ultraschallwandlern *Acustica* **36** 209–13

Herzfeld G and Litovitz T A 1959 *Absorption and Dispersion of Ultrasonic Waves* (New York: Academic)

Javanaud C, Lond P and Rahalkar R R 1986 Evidence for sound absorption in emulsions due to differing thermal properties of the two phases *Ultrasonics* **24** 137–41

Kaatze U, Kühnel V, Menzel K and Schwerdtfeger S 1993 Ultrasonic spectroscopy of liquids. Extending the frequency range of the variable sample length pulse technique *Meas. Sci. Technol.* **4** 1257–65

Kaatze U, Lautscham K and Brai M 1988 Acoustical absorption spectroscopy of liquids between 0.15 and 3000 MHz: II. Ultrasonic pulse transmission method *J. Phys. E: Sci. Instrum.* **21** 98–103

Kaatze U, Pottel R and Wallusch A 1995 A new automated waveguide system for the precise measurement of complex permittivity of low-to-high-loss liquids at microwave frequencies *Meas. Sci. Technol.* **6** 1201–7

Kaatze U, Trachimow C, Pottel R and Brai M 1996 Broadband study of the scattering of ultrasound by polystyrene-latex-in-water suspensions *Ann. Phys., Lpz.* **5** 13–33

Kaatze U, Wehrmann B and Pottel R 1987 Acoustical absorption spectroscopy of liquids between 0.15 and 3000 MHz: I. High resolution ultrasonic resonator method *J. Phys. E: Sci. Instrum.* **20** 1025–30

Khimunin A S and Lvova E A 1983 On the diffraction effects in an ultrasonic interferometer *Acustica* **53** 107–22

Kononenko V S 1987 Precision method for measurements of the ultrasound absorption coefficient in liquid at frequencies of 0.1–20 MHz *Sov. Phys.–Acoust.* **33** 401–4

Kühnel V 1995 Ultraschallabsorptionsspektroskopie im Frequenzbereich von 200 kHz bis 5 GHz an wäßrigen Lösungen symmetrischer Tetraalkylammoniumbromide *Dissertation* Universität Göttingen

Labhardt A and Schwarz G 1976 A high resolution and low volume ultrasonic resonator method for fast chemical relaxation measurements *Ber. Bunsenges. Phys. Chem.* **80** 83–92

Litovitz T A and Davis C M 1965 Structural and shear relaxation in liquids *Physical Acoustics* vol 2A, ed W P Mason (New York: Academic)

McClements D J 1992 Comparison of multiple scattering theories with experimental measurements in emulsions *J. Acoust. Soc. Am.* **91** 849–53

Menzel K, Rupprecht A and Kaatze U 1997 Broad-band ultrasonic spectrometry of C_iE_j/water mixtures. Precritical behaviour *J. Phys. Chem.* B **101** 1255–63

Sarvazyan A P 1982 Development of methods of precise measurements in small volumes of liquids *Ultrasonics* **20** 151–4

Schröder A and Raphael E 1992 Attenuation of ultrasound in silicone-oil-in-water emulsions *Europhys. Lett.* **17** 565–70

Slutsky L J 1981 Ultrasonic relaxation spectroscopy *Methods of Experimental Physics* vol 19, ed P D Edmonds (New York: Academic)

Strehlow H 1992 *Rapid Reactions in Solution* (Weinheim: Verlag Chemie)

Stuehr J E 1986 Ultrasonic methods *Investigations of Rates and Mechanisms of Reactions* ed C F Bernasconi (New York: Wiley)

Tamm K 1961 Schallabsorption und -dispersion in wäßrigen Elektrolytlösungen *Handbuch der Physik* vol 11/1, ed S Flügge (Berlin: Springer)

Trachimow C 1994 Ultraschallabsorptionsspektroskopie an wäßrigen Systemen mit kugelförmigen Einschlüssen: Polystyrol-Latex und 1,4-Diazabicyclo[2,2,2]oktan *Diplomarbeit* Universität Göttingen